AN OPERATIONAL PROCEDURE TO ESTIMATE THE FRAGMENTATION EPOCH FROM A SINGLE FRAGMENT OBSERVATION

M. F. Montaruli[(1)], P. Di Lizia[(1)], E. Cordelli[(2)], Hélène Ma[(3)], and J. Siminski[(4)]

[(1)]*Politecnico di Milano, Department of Aerospace Science and Technology (DAER), Via G. La Masa 34, 20156, Milan, Italy, Email: {marcofelice.montaruli, pierluigi.dilizia}@polimi.it*
[(2)]*GMV@ESA, Space Debris Office (SDO), European Space Operations Centre (ESA/ESOC), Robert-Bosch-Str. 5, 64293 Darmstadt, Germany, Email: emiliano.cordelli@ext.esa.int*
[(3)]*RHEA System GmbH@ESA, Space Debris Office (SDO), European Space Operations Centre (ESA/ESOC), Robert-Bosch-Str. 5, 64293 Darmstadt, Germany, Email: helene.ma@esa.int*
[(4)]*European Space Agency – European Space Operations Centre (ESA/ESOC), Robert-Bosch-Str. 5, 64293 Darmstadt, Germany, Email: jan.siminski@esa.int*

ABSTRACT

In the last decades, the growing in-orbit population of resident objects has become one of the main concerns for space agencies and institutions worldwide, and several initiatives have been promoted to tackle this issue. In the resulting Space Surveillance and Tracking services, orbiting objects are observed to assess possible conjunctions, and monitor satellite re-entry and fragmentations. Particular interest is attributed to fragmentation events, which can be due either to satellite collisions or explosions, as they further contribute to increase the number of space debris. In this context, orbiting objects are observed through ground-based sensors, which are radars, optical telescopes and laser stations. In particular, ground-based surveillance radars can generate measurements of an object that enters its field of view, which is pointed to survey specific regions. Thus, they do not need pass prediction to track the target, and an Initial Orbit Determination (IOD) problem is typically solved from a single measurement track if the observed object is uncatalogued. During fragmentations they can be used to reconstruct the orbital state of fragments if the observation is properly planned, which is paramount to update the space objects catalogue. For this purpose, the last available ephemeris of the parent object could be used to select the radar pointing and to schedule the acquisition time, although this procedure would allow to detect those fragments with orbits similar to the parent one. To implement a more effective observation strategy, the fragmentation epoch must be determined as soon as possible to apply break-up models, predict fragments cloud evolution and plan additional observations. Several past works have addressed the issue of identifying the fragmentation epoch, but they generally relied on the availability of ephemerides of many fragments, and they dealt with the problem in a deterministic way. On the contrary, even the availability of the orbital estimate of only one fragment could be leveraged to identify the fragmentation epoch, and the effect of the associated uncertainty cannot be neglected. The Fragmentation Epoch Detector (FRED) algorithm presented in this work has been developed to determine the fragmentation epoch through a statistical approach, starting from the last available ephemeris of the parent object and the fragment orbital state, which is reconstructed from surveillance radar measurements through an IOD process. The algorithm provides a set of fragmentation epoch candidates, ranked according to a statistical index, which is computed by assessing the similarity between the Minimum Orbital Intersection Distance (MOID) distribution and the relative distance one, the latter evaluated at the epoch of parent transit through the MOID. At the end, the candidate featuring the best index is considered as the optimal candidate solution. The work presents FRED algorithm, and a numerical analysis is conducted to assess its performance.

Keywords: Fragmentations; Initial Orbit Determination; Space Surveillance and Tracking; Surveillance radar; Minimum Orbital Intersection Distance.

1. INTRODUCTION

Space pollution has become a major concern for space agencies and institutions all around the world. Currently, about 9780 objects are orbiting around the Earth, but only 6900 are active [16]. Space Surveillance and Tracking (SST) programs are in charge of managing the challenges posed by the space traffic control problem.
Space debris are all artificial objects including fragments and elements thereof, in Earth orbit or re-entering the atmosphere, that are non functional [17]. Their presence may jeopardise the operative mission of active satellites, given that the possible impact with a space debris ranges from cumulative erosion of satellite surface, for debris smaller than 0.1 mm, to the possible satellite destruction, with the generation of thousands of additional pieces of

debris and inevitable environmental drawbacks and possible cascade effects [5]. In this context, about 640 break-ups, explosions, collisions, or anomalous events resulting in fragmentation have been recorded from the beginning of the space activities, which have further contributed to increase the number of space debris [16]. Therefore, it is fundamental to predict the fragments cloud evolution, in order to assess possible collisions, and, for this reason, the event epoch shall be identified as soon as possible.
Multiple works have been carried out in the past to deal with the fragmentation epoch identification, such as [11], [9], [12], [4], but all of them need numerous accurate ephemerides, and this is a quite optimistic assumption for multiple reasons, such as few observation data, problems in correlation procedure and Initial Orbit Determination (IOD) inaccuracy. Nevertheless, a prompt knowledge of the fragmentation epoch would be fundamental to plan additional observations of the fragments cloud and also to refine the processing of the observation measurements, aiming at obtaining more and more accurate orbit determination results. This would lead to also refine the estimation of the fragmentation epoch and, so, a virtuous circle would be generated.
The aim of the present work is to provide an operational procedure to estimate the fragmentation epoch starting from the last available ephemeris of the parent object (assumed as a deterministic quantity) and a single fragment orbital state provided with uncertainty. The latter is considered as determined by a surveillance radar, which allows to run IOD from a single observation with no transit prediction. To accomplish this purpose, the FRagmentation Epoch Detector (FRED) algorithm, implementing a statistical approach, has been developed.

2. FRAGMENTATION EPOCH DETECTOR - FRED

Let's consider the fragmentation of a space object whose last available ephemeris $\boldsymbol{x}^p$ is dated to t_{eph}, and is considered as a deterministic information. The event has occurred at $t_0 > t_{eph}$ and the related alert has been notified at $t_a > t_0$. Some hours later, one fragment is detected by a surveillance radar at t_{obs} (with $t_{obs} > t_a$) and its orbital state $\{\boldsymbol{x}^{fg}, \boldsymbol{P}^{fg}\}$ is first determined, where the mean $\boldsymbol{x}^{fg}$ and covariance $\boldsymbol{P}^{fg}$ are directly derived from the IOD process.
Since the orbit determination uncertainty cannot be a-priori neglected, FRED algorithm deals with the fragmentation epoch identification problem through a statistical approach, starting from a Monte Carlo distribution of the orbit determination result. Ideally, at the fragmentation epoch, both the Minimum Orbital Intersection Distance (MOID) [3] and the relative distance between the parent and the fragment are expected to be zero. In practical cases neither MOID nor relative distance turns out to be null, but they should statistically match each other. Therefore, the correct fragmentation epoch is expected to feature a matching between the MOID and the relative distance distributions.

FRED algorithm is structured as follows.

1. In order to include the fragment state uncertainty in the event epoch identification, a multinormal distribution of N_s [6] is created from the orbital state $\{\boldsymbol{x}^{fg}, \boldsymbol{P}^{fg}\}$.

2. The time window $[t_{eph}, t_a]$ is sampled with frequency $1/T^p$ (where T^p is the parent orbital period). This results in the epochs t_i, whose number is n_{orb}.

3. Both parent and fragment samples orbital states are propagated to each t_i.

4. For each t_i and for each j-th fragment sample, the epochs of transit through the MOID of both the parent and the fragment j-th sample are computed with a numerical scheme embedding [3], and indicated as t_j^p and t_j^s.
   This iterative process results in $N_s \times n_{orb}$ couples of $\left(t_j^p,\ t_j^s\right)$ and $\left(\boldsymbol{x}^p(t_j^p),\ \boldsymbol{x}^s(t_j^s)\right)$. It is important to observe that the difference between $\boldsymbol{p}^s(t_j^s)$ and $\boldsymbol{p}^p(t_j^p)$ (the $\boldsymbol{x}^s(t_j^s)$ and $\boldsymbol{x}^p(t_j^p)$ positions) allows to compute the 3-dimensional MOID: $\boldsymbol{m_j} = \boldsymbol{p}^s(t_j^s) - \boldsymbol{p}^p(t_j^p)$.

5. The fragment j-th sample state vector $\boldsymbol{x}^s(t_j^s)$ is propagated up to the epoch of parent transit through the MOID, resulting in $\boldsymbol{x}^s(t_j^p)$. It is worth to observe that the difference between the $\boldsymbol{p}^s(t_j^p)$ (the $\boldsymbol{x}^s(t_j^p)$ position) and $\boldsymbol{p}^p(t_j^p)$ provides the 3-dimensional relative distance between the j-th sample and the parent, at the epoch of parent transit through the MOID: $\boldsymbol{\rho_j} = \boldsymbol{p}^s(t_j^p) - \boldsymbol{p}^p(t_j^p)$.

6. All the n_{filter} epochs t_j^p are clustered according to a Density-Based Spatial Clustering of Applications with Noise (DBSCAN) [1]. From this operation, n_{cl} are identified. Fig. 1a presents the obtained clusters, in the plane t_j^p (in Coordinated Universal Time, UTC) versus scalar MOID.

7. For each n-th cluster, the candidate fragmentation epoch t_n^{fg} can be computed (in terms of mean and standard deviation) from the distribution of the epoch of parent transit through the MOID, which is indicated as F, and which is represented in Fig. 1b (for the correct cluster). In addition, $\boldsymbol{M}$ and $\boldsymbol{R}$ distributions (grouping the $\boldsymbol{m_j}$ and $\boldsymbol{\rho_j}$ respectively) are associated to each cluster. Fig. 2 shows the two distributions in Earth-Central-Inertial (ECI) reference frame, both for the correct candidate and for a not-correct one.

8. Afterwards, for each cluster:

   (a) All the $\boldsymbol{m_j}$ and $\boldsymbol{\rho_j}$ are rotated in the Modified Equidistant Cylindrical (EQCM) reference frame [8]. This operation results in MOID and relative distance distributions like in Fig. 3.

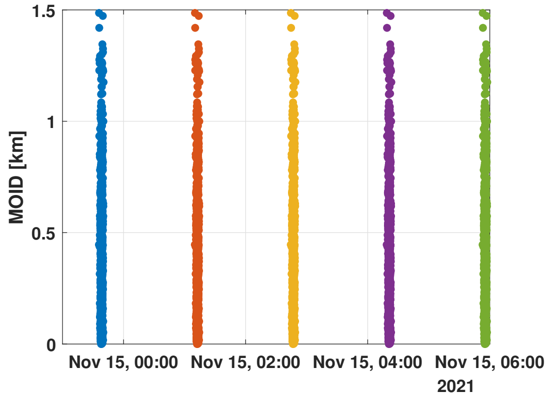

(a) Distribution of the t_j^p epochs in the time window of the analysis.

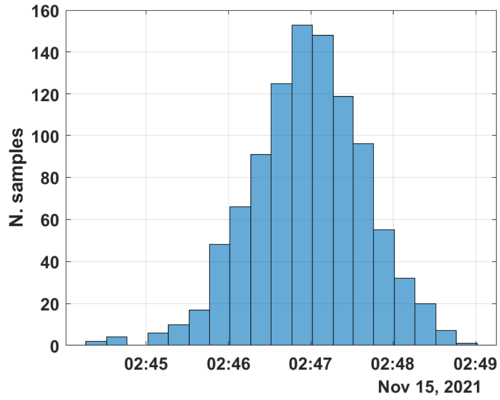

(b) Distribution of the t_j^p epochs for the cluster related to the correct solution.

Figure 1: Result of the clustering phase. The epochs are reported in UTC.

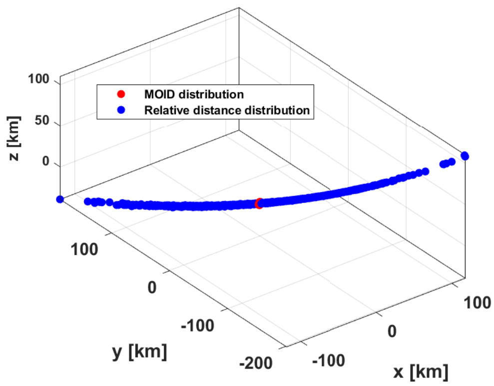

(a) Cluster related to the correct fragmentation epoch.

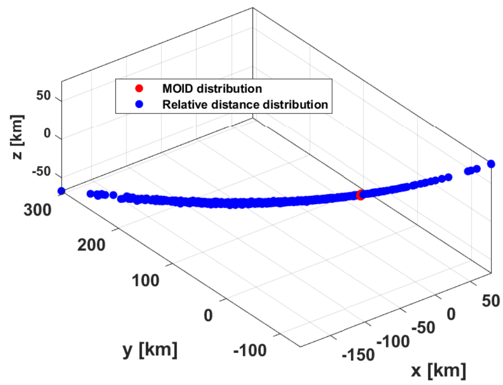

(b) Cluster related to a wrong fragmentation epoch.

Figure 2: $\boldsymbol{M}$ and $\boldsymbol{R}$ distributions in ECI reference frame, for the correct cluster and a non-correct one.

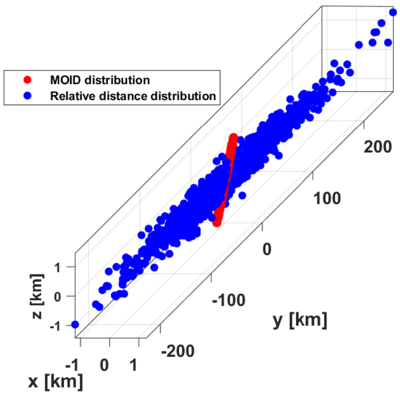

(a) Cluster related to the correct epoch.

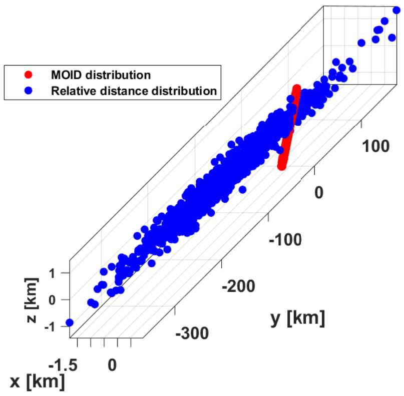

(b) Cluster related to a wrong epoch.

Figure 3: $\boldsymbol{M}$ and $\boldsymbol{R}$ distributions in EQCM reference frame, for the correct cluster and a not-correct one.

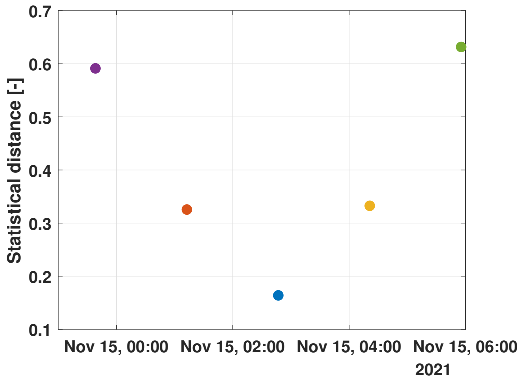

Figure 4: EMD statistical distance computed for each cluster.

(b) To be as generic and agnostic as possible regarding the distributions characteristics, the Earth Mover's Distance (EMD) [20] is selected to compare $\boldsymbol{M}$ and $\boldsymbol{R}$ for each cluster, as it is suitable for the non-Gaussian case as well. The implementation from [15] is used.

9. Repeating the operations above for each cluster results in Fig. 4, which shows the statistical distance in function of the F distribution mean. Finally, the cluster featuring the minimum statistical distance between the $\boldsymbol{M}$ and $\boldsymbol{R}$ distributions is selected, and the fragmentation epoch is returned from the related distribution F, in terms of mean and standard deviation.

3. NUMERICAL SIMULATIONS

A numerical simulation is here conducted to test the algorithm described in Sec. 2. The fragmentation scenario is the one which involved the Russian satellite COSMOS 1408 during the kinetic anti-satellite (ASAT) test which occurred around 02:47 UTC of November 15th, 2021 [7]. The ASAT test took place when the satellite was flying over the north-west Russia and the sensors of the European Space Surveillance and Tracking consortium [10] observed fragments generated by such an event.
The data set to test FRED algorithm is generated as follows:

1. The last available COSMOS 1408 ephemeris before the event are retrieved from the last TLE (Two-Line Elements) available on Spacetrack, which are dated to 00:55 UTC of November 15th [18]. To make the analysis time window more symmetrical with respect to the break-up event, they are propagated one orbital period back to the 23:20 UTC of November 14th, and the orbital state at this epoch is considered as $\boldsymbol{x_p}$.

2. The state vector $\boldsymbol{x_p}$ is propagated up to 02:47:00 UTC of November 15th. The fragmentation event is modelled as a series of impulses applied to the satellite orbital state at 02:47 UTC. These impulses are retrieved from the NASA standard break-up model [13]. A data set of 209 fragments is generated by this way.

3. The obtained ephemerides, representing the fragments, are propagated through SGP4 [14] until the epoch t_{obs}, when they are detected by a surveillance radar, and the orbital states $\left\{\boldsymbol{x}^{fg}, \boldsymbol{P}^{fg}\right\}$ are determined.

By this way all the inputs for the process described in Sec. 2 are obtained and FRED algorithm can be tested, considering an analysis time window ranging from 23:20 UTC of November 14th (epoch of the simulated last available ephemeris of the parent object) to 06:00 UTC of November 15th, retracing the fact that the COSMOS 1408 fragmentation alert was provided in the early morning (considering UTC coordinates). These two epochs correspond to t_{eph} and t_a introduced in Sec. 2. The t_{obs} is set 13 h after the event, as the method aims at reconstructing the fragmentation epoch from a single fragment observation conducted in the hours right after the event.
Based on this data set, FRED is run on each fragment IOD result $\left\{\boldsymbol{x}^{fg}, \boldsymbol{P}^{fg}\right\}$ separately, considering 1000 samples for the multinormal distribution, as well as a SGP4 propagation [14]. The IOD process is simulated as run from measurements acquired by a surveillance radar, which, collecting both angular and slant range measurements with no need of pass prediction, allows to initially determine the orbit without other sensor contributions.
The state vectors retrieved from the fragmentation are propagated for 13 h, and measurements are synthetically generated, for a radar receiver simulated at the fragment nadir, which are azimuth, elevation and range. A Gaussian noise is then added, with standard deviations of 30 m for the range and 0.01 deg for Azimuth and Elevation, coherently with what presented for the Bistatic Radar for LEO Survey (BIRALES) in [2]. BIRALES characteristics are taken as reference because it was one of the most contributing sensors in the European Space Surveillance and Tracking consortium [10] which observed fragments generated by COSMOS 1408. Starting from the measurements, the IOD is performed according to the procedure described in [19], and the fragment orbital state $\left\{\boldsymbol{x}^{fg}, \boldsymbol{P}^{fg}\right\}$ at the observation epoch t_{obs} is obtained.
For a single fragment analysis, the result is considered successful if the difference between the epoch estimation and the correct value (t_{err}) is below 60 s in the analysis.
FRED failures can be linked to either the MOID computation (if parent and fragment sample orbits are similarly oriented) or to the distributions comparison performed through the EMD (if they share a similar orbital period), and for this reason they are classified as follows:

- MOID failures - compliant: 1 min. $< t_{err}$ and $t_{err} < 3\sigma_t$, where σ_t is the standard deviation associated to the F distribution. An erroneous estimation of the parent transit through the MOID occurs, but the distribution is wide enough to include such an error.

- MOID failures - uncompliant: 1 min. $< t_{err}$ and $3\sigma_t < t_{err} < T^p/2$. The erroneous estimation of the epoch is not mitigated by its uncertainty, with an error smaller than the half of the parent orbital period.

- EMD failures: $t_{err} > T^p/2$. In these cases, the statistical comparison identified a not-correct cluster and, so, a wrong candidate is returned as result.

The results are reported in Tab. 1 and represented in Fig. 5a. They are more better than those reported in Tab 2 and represented in Fig. 5b, which are related to the fragmentation epoch estimation assessed through a relative distance metrics, that is performed by assessing the fragmentation epoch as the time of the minimum relative distance between the parent and the fragment mean state (both assumed as deterministic), propagated on the analysis time window. Besides being more performing, in FRED the correct solution is present among the candidate clusters even when a failure occurs, while this is not the case for the relative distance metrics.

4. CONCLUSIONS

The paper described FRED algorithm, which detects the fragmentation epoch through a statistical method which starts from the IOD result of a single fragment and the last available parent ephemeris. The numerical simulations highlighted that FRED represents a possible choice in operational scenarios. The prompt estimation of the fragmentation epoch through a statistical model from the observation of a single fragment would generate a virtuous circle, leading to better monitor the fragment cloud evolution.
In the future, FRED algorithm will be further validated through both synthetic and real data.

ACKNOWLEDGMENTS

The research activities described in this paper were performed within the European Commission Framework Programme H2020 and Copernicus "SST Space Surveillance and Tracking" contracts N. 952852 (2-3SST2018-20) and N. 299-G-GRO-COPE-19-11109 (1SST2018-20) and the support of the Italian Space Agency through the grant agreement n. 2020-6-HH.0 (Detriti Spaziali – Supporto alle attività IADC e SST 2019-2021).

REFERENCES

1. Ester M., Kriegel H.-P., Sander J., Xu X., (1996). A Density-Based Algorithm for Discovering Clusters in Large Spatial Databases with Noise, AAAI Press
2. Montaruli M.F., Facchini L., Di Lizia P., Massari M., Pupillo G, Bianchi G., Naldi G., (2022). Adaptive track estimation on a radar array system for space surveillance, Acta Astronautica
3. Gronchi G. F., (2005). An Algebraic Method to Compute the Critical Points of the Distance Function Between Two Keplerian Orbits, Journal of Celestial Mechanics and Dynamical Astronomy
4. Romano M., Muciaccia A., Trisolini M., Di Lizia P., Colombo C., Di Cecco A., Salotti L., (2021). Characterising in-orbit fragmentations with the PUZZLE software, 8th International Conference on Astrodynamics Tools and Techniques (ICATT)
5. Kessler D. J., Cour-Palais B. G., (1978). Collision frequency of artificial satellites: The creation of a debris belt, Journal of Geophysical Research
6. Kotz S., Balakrishnan N., Johnson N. L., (2000). Continuous Multivariate Distributions. Models and Applications, New York: John Wiley
7. EUSST, (2022). COSMOS 1408 fragmentation. Available online at: `https://www.eusst.eu/newsroom/eu-sst-confirms-fragmentation-cosmos-1408/`
8. Vallado D., Alfano S., (2014). Curvilinear coordinate transformations for relative motion, Celestial Mechanics and Dynamical Astronomy
9. Frey S., Colombo C., Lemmens S., (2018). Density based modelling and indication of break-up location and epoch from fragments using backwards propagation, 5thEuropean Workshop on Space Debris Modelling and Remediation
10. EUSST, (2022). European Space Surveillance and Tracking website. Available online at: `https://www.eusst.eu/`
11. Andrisan R. L.,Ioniţă A., Domínguez González R., Sánchez Ortiz N., Pina Caballero F., Krag H., (2016). Fragmentation Event Model and Assessment Tool (FREMAT) Supporting On-Orbit Fragmentation Analysis, 7th European Conference on Space Debris
12. Di Mare L., Cicalò S., Rossi A., Alessi E. M., Valsecchi G. B, (2019), In-Orbit Fragmentation Characterization and Parent Bodies Identification by Means of Orbital Distances, First International Orbital Debris Conference
13. NASA, (2011). Proper implementation of the 1998 NASA breakup model, Orbital Debris Quarterly News
14. Vallado D.A., Crawford P., Hujsak R., Kelso T.S., (2006), Revisiting Spacetrack Report #3, AIAA Astrodynamics Specialists Conference and Exhibit
15. SciPy, (2022). SciPy documentation, Available online at: `https://docs.scipy.org/doc/scipy/`

Correct solutions	MOID failures - compliant	MOID failures - uncompliant	EMD failures
68.9 %	9.6 %	0.5 %	21.0 %

Table 1: Operational scenario: FRED results.

Correct solutions	1 minute $< t_{err} < T^p/2$	$t_{err} > T^p/2$
12.4 %	67.0 %	20.6 %

Table 2: Operational scenario: relative distance metrics results.

16. ESA, (2022). Space debris by the numbers. Available online at: https://www.esa.int/Space_Safety/Space_Debris/Space_debris_by_the_numbers

17. Inter-Agency Space Debris Coordination Committee, (2022). Space Debris Mitigation Guidelines

18. Space-track, (2021). Space-track website, Available online at: https://www.space-track.org/auth/login

19. Siminski J., (2016). Techniques for assessing space object cataloguing performance during design of surveillance systems, in Proc. 6th International Conference on Astrodynamics Tools and Techniques (ICATT)

20. Levina E., Bickel, P., (2001). The Earth Mover's distance is the Mallows distance: some insights from statistics, Proceedings Eighth IEEE International Conference on Computer Vision

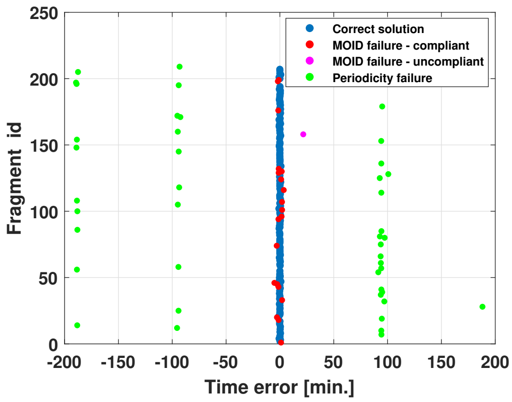

(a) Time error for each fragment of the data set by using FRED algorithm.

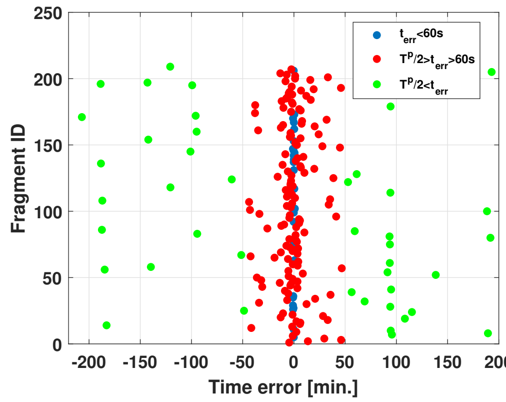

(b) Time error for each fragment of the data set by using the minimum relative distance metrics.

Figure 5: Fragmentation epoch estimation error. The fragments for which a failure occurs are highlighted according to the legend.